The British Journal of Radiology, 73 (2000), 376–383

Quality assurance for MRI: practical experience

[1,2]M J FIRBANK, PhD, [2]R M HARRISON, PhD, [3]E D WILLIAMS, PhD, FIPEM and [1]A COULTHARD, FRCR

[1]*University Department of Radiology, Royal Victoria Infirmary, Newcastle upon Tyne NE1 4LP,* [2]*Regional Medical Physics Department, Newcastle General Hospital, Newcastle upon Tyne NE4 6BE and* [3]*Regional Medical Physics Department, Sunderland Royal Hospital, Kayll Road, Sunderland SR4 7TP, UK*

Abstract. The aim of this study is to propose guidelines for quality assurance (QA) in MRI, based on a comprehensive assessment of QA parameters undertaken on a busy clinical MRI scanner over the course of 1 year. QA phantoms supplied by the scanner manufacturer were used together with the Eurospin MRI phantom set. Signal-to-noise ratio (SNR) and image uniformity were measured daily from spin echo images acquired using a quadrature send–receive head coil and from a gradient echo sequence using the Helmholtz body coil. The voltage of the transmit radiofrequency (RF) amplifier was noted. Monthly measurements of slice thickness, geometric distortion, slice position, image resolution and image ghosting were acquired using the head coil. In addition, SNR was measured monthly on a selection of commonly used coils. Apart from some drift of the RF amplifier voltage, all measurements were within acceptable limits and were stable over the course of 1 year. Satisfactory measurements of SNR were possible using the simple phantom supplied with the scanner. The SNR, geometric distortion and RF amplifier voltage are simple to determine and can be measured in less than 15 min by the scanner operator, using the scanner software. Weekly recording of these parameters is recommended for busy clinical MRI scanners, as this should allow deviations from acceptable limits to be identified early. Such in-house checks can usefully be compared with the less frequent estimations performed by the service engineer. Comprehensive QA routines are discussed for systems used for quantitative measurements.

Quality assurance (QA) in imaging can involve regular monitoring of a portfolio of measurements to determine compliance with acceptable limits. The purpose of such monitoring is to detect changes in performance before they can adversely affect clinical images. QA programmes for imaging techniques using ionizing radiation and ultrasound are well established [1–4]. Whilst measurements that might be useful as part of a QA programme for MRI have been described [5–8], there is a scarcity of guidelines to MRI users as to what would constitute an acceptable QA schedule. Most MRI units have heavy demands on scanning time and it would be desirable to keep the frequency and duration of QA testing to a minimum. The purpose of this study was to use practical experience to define a set of QA guidelines for MRI acceptable for use in a busy clinical setting.

Methods

A programme of frequent QA measurements was established over the course of 1 year. All measurements were performed on a 1.0 T superconducting magnet (Siemens Impact Expert, Siemens, Erlangen, Germany). Two sets of phantoms were used. Table 1 describes the set of quality assurance phantoms supplied with the magnet by the manufacturers. The Eurospin test objects (Diagnostic Sonar, Livingston, Scotland) were also used [5]. An additional simple phantom was constructed in-house to measure ghosting. This consisted of a small plastic bottle positioned off-centre in both *x*- and *y*-axes within a polystyrene disc (Figure 1). The bottle contained a dilute solution (3 mmol) of $CuSO_4$. All phantoms were stored in the scanner room. Room temperature was recorded at the time of QA measurements using an alcohol thermometer.

Signal-to-noise ratio

Signal-to-noise ratio (SNR) is a sensitive, although non-specific, monitor of the status of the MRI system [5, 7]. SNR was measured using the Siemens phantoms (Table 1). The spherical design of the head and body phantoms allowed images to be obtained in orthogonal planes without re-adjusting the position of the phantom. The $NiSO_4$ solution within the Siemens phantom

Received 11 August 1999 and in revised form 4 November 1999, accepted 19 November 1999.

Table 1. Description of the Siemens quality assurance phantoms

	Composition (per 1000 g H_2O)	Description	Used for
Head phantom	1.25 g $NiSO_4$•$4H_2O$	Sphere, 180 mm (outer diameter), 170 mm (inner diameter)	Head coil
Head annulus	2 g NaCl 3 g $MnCl_2$•$4H_2O$	Cylindrical annulus 230 mm diam., 400 mm long	
Body phantom	1.25 g $NiSO_4$•$4H_2O$	300 mm sphere and annulus	Body coil
Body annulus	5 g NaCl 3 g $MnCl_2$•$4H_2O$	Oval annulus 300 mm × 400 mm diameters, 530 mm long	Body coil
Spine phantom	1.25 g $NiSO_4$•$4H_2O$ 5 g NaCl	Flat rectangular phantom (400 mm × 150 mm × 50 mm)	Spine coil
Small phantom	1.25 g $NiSO_4$•$4H_2O$ 5 g NaCl	1 l bottle (100 mm diameter)	Knee, neck, breast, flex coils

has a T_1 value approximately half that of the Eurospin phantom, allowing use of a shorter repetition time (TR) and therefore reduced scanning time. T_1 of the $NiSO_4$ solution is also more stable with temperature than the $CuSO_4$ solution contained within the Eurospin phantom [5]. Loading annuli were used for the head and body coils. The phantoms used for the other coils contained dilute NaCl in order to provide resistive coil loading (Table 1).

To calculate SNR the following method was used [9, 10]. An image of the phantom was acquired using the relevant sequence, shown in Table 2. Using the scanner software, a large circular region of interest (ROI) was positioned so that it encompassed most of the image of the test object. The mean signal intensity (I) was noted. An estimation of noise was derived from the standard deviation of the pixel values in a small circular ROI (approx. 20 mm radius = 1300 pixels) placed on the air surrounding the phantom (SD_{air}). The noise was not taken from the image of the phantom, since the variation in signal intensity owing to non-uniformity is larger than that owing to random noise. Care was taken to avoid placing the air ROI over ghosting artefacts or other regions of non-uniformity. The SNR in this case is given by:

$$\mathrm{SNR} = 0.655 \frac{I}{\mathrm{SD}_{\mathrm{air}}} \qquad (1)$$

The correction factor (0.655) arises because noise is normally distributed about zero. Fourier transformation and construction of a magnitude image (*i.e.* with no negative values) results in a skewed distribution for noise and the 0.655 compensates for this [9]. The SNR was measured on a daily basis on the head coil (send–receive quadrature coil) and the body coil (Helmholtz coil). It was measured monthly on other frequently used coils. Uniformity and geometric distortion were also estimated from the image used for SNR (see Appendix). On our scanner it is possible to display on the console the resonant frequency and the voltage of the transmit radiofrequency (RF) (valve) amplifier used during the scan. These were recorded whilst the phantoms were being scanned in the head and body coils to check for any system changes.

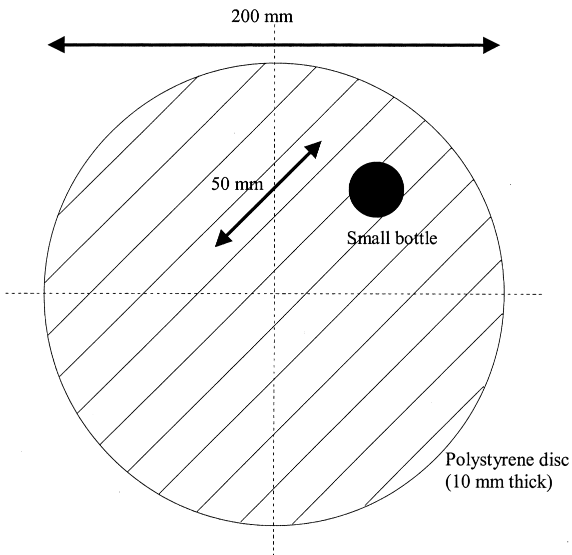

Figure 1. Schematic diagram of phantom used to measure ghosting artefact.

Other parameters

Other parameters measured were image uniformity, slice profile and thickness, slice position, ghosting, geometric distortion and spatial resolution. Protocols for measuring these parameters were adapted from published methods [5–7] and are described in detail in the Appendix. The analysis was carried out either on the scanner console or offline, using the "Dispimage" image display package, available at low cost (Dispimage: Department of Medical Physics, University College London [11]).

Table 2. Sequences used. All sequences had a bandwidth of 130 Hz per pixel. All sequences were spin echo apart from the body coil, which was a gradient echo FLASH (fast low angle shot) sequence

Coil	TE (ms)	TR (ms)	Slice thickness (mm)	Flip angle (°)	Matrix size	Orientation	FOV (mm)	Time (min:s)
Head	12	500	5	90	256×256	Ax,Cor,Sag	250	2:10
Body	6	60	10	40	256×256	Ax	300	0:16
Spine	30	1000	5	90	160×256	Cor	313	2:40
Breast	30	1000	5	90	128×256	Cor	250	2:10
Knee, neck, flex coils	30	1000	5	90	128×128	Ax	125	2:10

TE, echo time; TR, repetition time; FOV, field of view. Ax, axial; Cor, coronal; Sag, sagittal.

Results

Signal-to-noise ratio

Repeated measurement (n=15) of SNR on the same day gave a value of 80.6 (SD=1.45). The variation of T_1 of $NiSO_4$ with temperature is negligible, but SNR is still temperature dependent, being affected by the resistive loading of the receiver coil [12]. The resistive loading is dependent on the conductance of the fluid within the annulus, which falls with increasing temperature. Figure 2 shows measured SNRs plotted against room temperature. The ambient room temperature varied from 17 ℃ to 23 ℃; the point at 7 ℃ was measured after cooling the phantom (and thermometer) in a refrigerator. From this graph, the variation of SNR with temperature T was calculated thus:

$$\mathrm{SNR} = 94.1 - 0.766T \qquad (2)$$

Equation 2 was used to calculate mean values for different temperatures, and these figures were subtracted from measured SNR to give temperature corrected values ($\mathrm{SNR_{TC}}$). Figure 3 shows the variation of $\mathrm{SNR_{TC}}$ with time for the head coil. As can be seen from this figure, $\mathrm{SNR_{TC}}$ has been relatively stable over the period of study. The body coil SNR also remained similarly stable, as did the SNR measured on a monthly basis on the other coils.

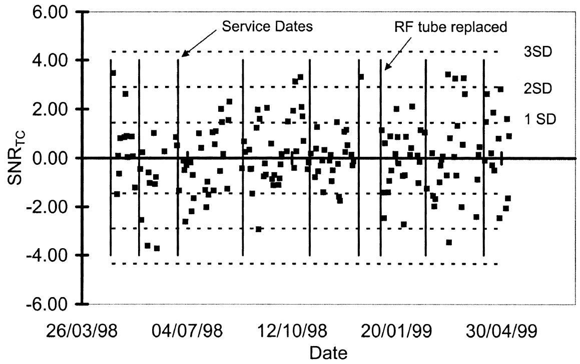

Figure 3. Change in temperature-corrected signal-to-noise ratio ($\mathrm{SNR_{TC}}$) on the head coil with time. The dates of services of the scanner are shown as vertical solid lines. Horizontal dotted lines show ±1, 2 and 3 SD of measurement.

Figure 3 also shows the dates of the scanner services (as vertical lines). There is evidence of drift in SNR between services, particularly between July and November 1998. Figure 4 shows $\mathrm{SNR_{TC}}$ between 25 June 1998 and 24 August 1998. A linear regression of the data has a slope of 0.04 per day. Over the 60 days shown, this corresponds to an average increase in $\mathrm{SNR_{TC}}$ of 2.4 (equal to 1.7 SD). A change of similar magnitude was seen on the body coil.

The RF transmit amplifier tube was replaced at the beginning of 1999. As a result of this

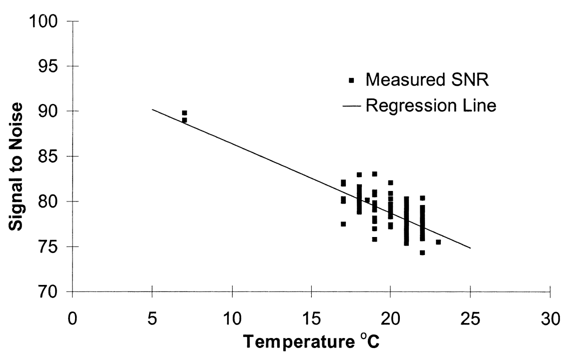

Figure 2. Signal-to-noise ratio against phantom temperature measured on the head coil. The regression line is shown.

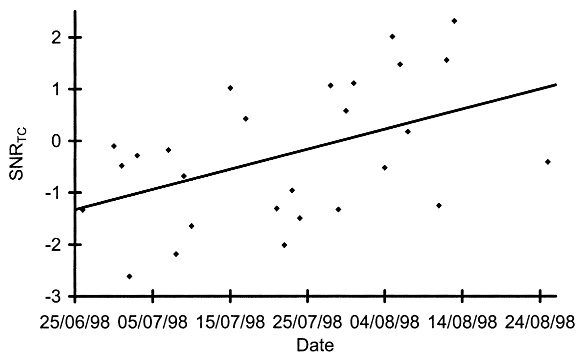

Figure 4. Temperature-corrected signal-to-noise ratio ($\mathrm{SNR_{TC}}$) in between service visits from 26 June 1999 to 25 August 1999. The regression line is shown.

replacement, SNR_{TC} increased by 0.88 (as measured by comparing an average of 50 points post change with all the points before the change). The data plotted in Figure 3 after 1 January 1999 have had 0.88 subtracted from them so that the fluctuations in SNR before and after the coil change can be easily compared. A smaller increase was seen on the body coil SNR (0.4%, compared with 1.1% for the head coil). The reason for a difference in the change in SNR in the body and head coils is uncertain. It might be because the RF transmit amplifier voltage for the head coil phantom is 55 V, whilst it is 255 V for the body coil phantom — it is possible that the voltage response of the new RF amplifier is slightly different to the old one. Since SNR on the other coils was only measured on a monthly basis, shifts of this small magnitude could not be detected in the given time-scale.

Figure 5 shows the changes in transmit RF amplifier voltage as measured on the body coil. The voltage measured immediately after the service visits (usually ~260 V) has been subtracted from subsequent values. Most changes were less than 5 V, though in April/May 1999 a larger drift was seen, and the service engineer was called. He confirmed that the RF amplifier characteristics had drifted and he made appropriate adjustments. No significant changes were seen in the SNR measurements on either the head or body coils, nor in the voltage measured on the head coil. Resonant frequency remained steady over the period of study, with a value of 40.6 MHz (SD=9 Hz).

Uniformity

Image uniformity [Equation (A1)] in the axial plane for the head coil was 0.89 (SD=0.008), 0.61 (SD=0.015) in the coronal plane and 0.70 (SD=0.015) in the sagittal plane. The uniformity remained constant in the sagittal and coronal planes, although the uniformity values are lower than in the axial plane owing to the quadrature

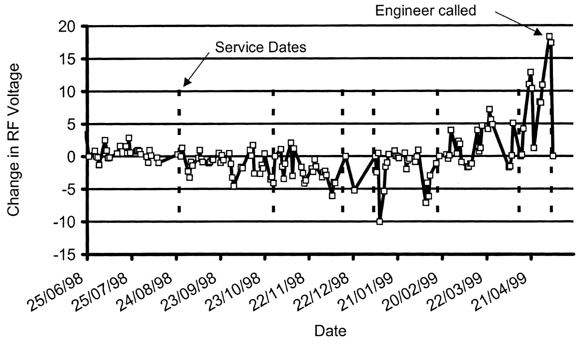

Figure 5. Change in voltage of radiofrequency (RF) tube from last service, measured on the body coil. Service dates are shown as vertical dotted lines.

design of the head coil. Image uniformity was also measured monthly on the other coils. Uniformity varied between coils but remained stable for any particular coil to within ±3SD.

Other parameters

All other parameters remained stable over 1 year. Table 3 shows a comparison of the average results from our scanner with suggested acceptance criteria [6, 7], with the Medical Devices Agency evaluation of the same model of scanner [13] and with the specifications stipulated by Siemens [14]. All parameters measured in this study meet the suggested criteria.

Figure 6 shows a typical 5 mm slice profile, showing that the slice width at 50% of maximum is nearly equal to the nominal value.

Overall results

The scanner SNR has remained constant over the study period, with all points falling within ±3 SD of the mean. The most rapid change in SNR over time was 2 SD over 2 months between services. The transmit RF amplifier voltage measured using the body coil showed a drift of 15 V over 2 weeks on one occasion. No significant change in SNR occurred over this period, and no significant change was seen in the voltage measured on the head coil. The other parameters measured fell within acceptable limits [6, 7, 13, 14] and remained stable with time.

Discussion

Role of different QA parameters

Drift in the transmit RF (valve) amplifier voltage may cause the flip angle to be incorrect since, for each patient, the RF amplifier voltage required to give a 90° flip angle is measured. This voltage acts as a reference for calculation of the voltages required for other flip angles. If the RF amplifier characteristics have changed, this calculation may be incorrect. A drift in amplifier voltage may also indicate that the RF amplifier is aging and needs to be replaced. Variations in the resonant frequency reflect changes in the magnetic field. The SNR is sensitive to most changes in system parameters. Change in slice thickness will affect the SNR, since the measured signal is proportional to the slice thickness. Errors in slice position will either be due to non-uniformity in the gradient field or main magnetic field [7]; these errors should also cause distortion in the SNR phantom. Changes in the pixel resolution should also lead to variations in SNR and distortion [15].

For a scanner in normal clinical use, regular monitoring of the SNR, geometric distortion,

Table 3. Acceptable errors in measurement as determined from the American Association of Physicists in Medicine (AAPM) report [7], from the manual supplied with the Eurospin test objects [6], from the typical values for our model of MR scanner from the MDA report [13], from the specifications given in the Siemens manual [14] and from the average values measured over the year in our study

Measured value	AAPM suggested action criteria	Eurospin manual suggested action criteria	Typical errors in MDA report for Siemens 1.0 T magnet	Siemens specification	Average errors on our system
Slice thickness	To within 1 mm	<10% error	⩽10%	Within 20%	<10%
Geometric distortion	<5% (over 25 cm)	<5%	<1% (over 120 mm)	Within 2.5%	<1% (120 mm) <2% (170 mm)
Ghosting	<5%	No specific value given	Minimal	—	⩽1% (only on 2nd/3rd echo)
Spatial resolution	Equal to pixel size	No specific value given	Within 10% of pixel size	Within 20% of pixel size	Within 10% of pixel size
Slice position	<20% (or <1 mm) error	<1 mm error	2% (over 160 mm)	—	Within 1% (over 33 mm)

uniformity and ghosting should be sufficient to detect drift of these other parameters from acceptable limits. Note that an increase in SNR is not necessarily good, since it may well be caused by deterioration of another parameter, for example an increase in the slice thickness. In an ideal situation, all these parameters should remain constant.

Time taken for measurements

Measurements of SNR, RF tube voltage, image uniformity and geometric distortion can be obtained from a single scan of a phantom using console software that allows ROI placement and produces basic image statistics. The total measurement time (including set-up and calculation) takes 10–15 min and could be performed by the operator of the scanner.

Analysis of ghosting can also be performed in a simple fashion, requiring 15–20 min to analyse all three orthogonal imaging planes. Accurate estimation of slice thickness, slice position and pixel resolution requires special phantoms, and additional software is needed to analyse the data. Each of these parameters takes 20–30 min per image plane for acquisition and analysis.

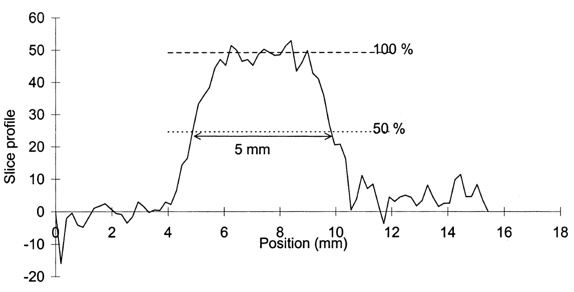

Figure 6. Typical 5 mm slice profile measured on the head coil in the axial plane using the Eurospin test object.

Frequency and analysis of measurements

The frequency of performing QA measurements depends in part upon the time available. From our data, the drift of RF voltage occurred over 2 weeks. The maximum drift in SNR measured was 2 SD over 2 months. Weekly measurements of SNR and RF tube voltage should therefore be sufficient to monitor system performance. No change in ghosting artefact was noted; monthly estimations of ghosting should be sufficient. If there is any gross change in ghosting, this will be evident on the image used for the SNR.

Monthly estimations of SNR on other frequently used coils will provide a baseline that may be used to demonstrate any damage that occurs to those coils.

Action criteria can be set through the use of control charts, *e.g.* plotting the data on a chart showing standard deviation lines and using standard quality control theory [16, 17]. Further investigation would be suggested if one point lies outside 3 SD, or two consecutive points lie outside 2 SD. An average of 5–10 SNR measurements should be used to set the baseline against which SNR measurements are compared. A running average of 5–10 points could be used to monitor the long-term drift of the SNR.

Baseline measurements of all the QA parameters discussed in this study may be useful as a reference for future measurements. After any major change to the scanner, it is useful to check whether the baseline values have shifted. Obviously, if there are any perceived changes in clinical images then these can be investigated by comparing phantom measurements against the baseline.

Practical considerations

Estimating SNR on a plug-in coil allows the electrical connections to be checked. However, because of the proximity of the head coil to the QA phantom, it is less sensitive to variations in the RF amplifiers; the body coil provides a more sensitive test of this. Ideally, we would suggest a combination of measurement of transmit RF amplifier voltage and resonant frequency on the body coil, and SNR, distortion and uniformity on the head coil. However, the RF amplifier tube is more likely to deteriorate than the coil connections, thus if a single phantom were to be used, we recommend using the body coil to take a single image to estimate SNR, distortion and uniformity, and recording the RF amplifier voltage and resonant frequency. It may be useful to measure the background signal in the phase-encoding direction on the SNR image to obtain an estimate of the ghost artefact.

Any phantom giving an image with a uniform area of signal can be used. Ideally, the QA phantom should have an annulus that simulates the conductive properties of a patient (such as the annulus supplied by Eurospin or Siemens). If the resistive loading of the phantom is not similar to that of a patient, the measured SNR will be unrealistically high (compared with SNR of clinical images), and system changes that affect clinical images may not have an obvious effect on the phantom measurement. Measurement of image uniformity is sensitive to the positioning of the ROI; a small region in the centre of the image will typically have a higher uniformity than a large ROI covering all of the image. It is thus necessary to be consistent both in size and position of the ROI. It is also important to record the phantom temperature so that temperature-induced changes can be distinguished from genuine system changes.

QA for quantitative measurements

If the images are to be used for quantitative measurements (*e.g.* of tumour volume or for radiotherapy planning), then geometric distortion, slice thickness and location will affect the measurements, and the actual values of these parameters should be measured in order to determine any error. It would be desirable to use a slice position phantom that covered a larger volume than the Eurospin TO3 (which is only 30 mm long). A more comprehensive geometric distortion phantom than Eurospin TO2, such as a grid of rods at regular intervals covering a large volume, might also be needed. If T_1 and T_2 values are to be measured, then the accuracy of these should be checked using the Eurospin gels or other materials with calibrated T_1 and T_2 values. If uniformity values are important, an oil phantom is recommended, since standing wave artefacts occur in large water phantoms but are negligible in oil [18]. The frequency of these additional tests will depend upon the frequency of the quantitative measurements.

Conclusion

SNR, transmit RF amplifier voltage, resonant frequency, image uniformity and geometric distortion can be simply measured from a single image of a uniform phantom in less than 15 min. We recommend that such a measurement be carried out on a weekly basis to provide assurance of consistent performance of clinical MRI systems.

Acknowledgments

We wish to thank R A Lerski (Dundee), N Lincoln (Siemens), L Moore (Southampton), T W Redpath (Aberdeen) and S Wayte (Coventry) for helpful advice on MR QA procedures.

References

1. The Institute of Physics and Engineering in Medicine. Recommended standards for the routine performance testing of diagnostic X-ray imaging systems, IPEM Report No. 77. York: IPEM, 1997.
2. The Institute of Physics and Engineering in Medicine. Quality control of gamma cameras and associated computer systems, IPEM Report No. 66. York: IPEM, 1997.
3. The Institute of Physics and Engineering in Medicine. Routine quality assurance of ultrasound imaging systems, IPEM Report No. 71. York: IPEM, 1995.
4. Hospital Physicists' Association (HPA) measurement of the performance characteristics of diagnostic X-ray systems used in medicine. Topic Group Report (TGR) 32 Part III: computed tomography X-ray scanners. York: IPEM, 1981.
5. Lerski RA, de Certaines JD. Performance assessment and quality control in MRI by eurospin test objects and protocols. Magn Reson Imaging 1993; 11:817–33.
6. Eurospin test object manual. Livingston, Scotland: Diagnostic Sonar Ltd., 1992.
7. Price RR, Axel L, Morgan T, Newman R, Perman W, Schneiders N, et al. Quality assurance methods and phantoms for magnetic resonance imaging: report of AAPM nuclear magnetic resonance task group no 1. Med Phys 1990;17:287–95.
8. Lerski RA, de Wilde J, Boyce D, Ridgeway J. Quality control in magnetic resonance imaging, IPEM Report 80. York: IPEM, 1995.

9. Kaufman L, Kramer DM, Crooks LE, Ortendahl DA. Measuring signal to noise ratios in MR imaging. Radiology 1989;173:265–7.
10. Firbank MJ, Coulthard A, Harrison RM, Williams EDA comparison of two methods for measuring the signal to noise ratio on MR images. Phys Med Biol 1999;44:N261–4.
11. Plummer DL. DispImage: a display and analysis tool for medical images. Riv Neuroradiol 1992;5: 489–95.
12. McRobbie DW. The absolute signal to noise ratio in MRI acceptance testing. Br J Radiol 1996;69: 1045–8.
13. Medical Devices Agency evaluation report No. MDA/97/45. Siemens Magnetom Impact Expert 1.0T MR imaging system. London: MDA.
14. Siemens MAGNETOM impact and impact expert guide VB31B. Erlangen: Siemens, 1996.
15. Hyde RJ, Ellis JH, Gardner EA, Zhang Y, Carson PL. MRI scanner variability studies using a semi-automated analysis system. Magn Reson Imaging 1994;12:1089–97.
16. Caplen RH. A practical approach to quality control. London: Hutchison Business, 1988.
17. Westgard JO, Barry PL, Hunt MR, Groth T. A multi rule Shewhart chart for quality control in clinical chemistry. Clin Chem 1981;27:493–501.
18. Simmons A, Tofts PS, Barker GJ, Arridge SR. Sources of intensity nonuniformity in spin echo images at 1.5 T. Magn Reson Med 1994;32:121–8.
19. Judy PF. The line spread function and modulation transfer function of a computed tomographic scanner. Med Phys 1976;3:233–6.
20. Steckner MC, Drost DJ, Prato FS. Computing the modulation transfer function of a magnetic resonance imager. Med Phys 1994;21:483–9.

Appendix

Uniformity

Image uniformity was measured from the image used for the signal-to-noise ratio (SNR) by constructing a large circular region of interest (ROI) covering 90% of the phantom, avoiding the edges (this was the same ROI as was used for the SNR calculation). Image uniformity U was defined as [7]:

$$U = 1 - \frac{\text{max.} - \text{min.}}{\text{max.} + \text{min.}} \tag{A1}$$

where max. and min. are the maximum and minimum pixel intensities in the region, respectively.

Slice profile and thickness

Slice thickness was measured using the Eurospin test object TO2, which contains two Perspex wedges and two angled plates, placed at an angle of 11.3° to the scanning plane. Images were acquired using the TR/TE 500/12 spin echo sequence, with 5 mm and 3 mm slice thickness in each of sagittal, coronal and axial planes. On the resultant images, line profiles 20 pixels wide through the wedges were drawn using the image display package Dispimage [11]. These profiles were exported as text files, and the distance was scaled by multiplying by tan (11.3)=0.2 and differentiated with respect to distance to give the slice profile.

The full width at half maximum (FWHM) of the slice profile was used as a measure of the slice thickness (Figure 6). Profiles were drawn on both angled wedges (which slope in opposite directions), and the FWHM calculated on both. The geometric mean of the two values was calculated to correct for any misalignment in the test object [7]. The slice thickness was measured on the head coil, weekly for 5 weeks and monthly thereafter.

Slice position

Slice position was measured using Eurospin TO3, which contains a number of crossed Perspex rods. 11 contiguous 3 mm slices were taken (TR/TE 500/12) in the coronal, sagittal and axial planes. The distances between four pairs of rods on each slice were measured using Dispimage. The mean distance was multiplied by a correction factor to give the slice position relative to the object centre. From a graph plotting measured position against required position, a regression fit was calculated using Excel (Microsoft). The slope thus calculated gave the error in position. Owing to the geometry of the phantom, the range of slice positions was limited to 33 mm.

Ghosting

Ghosting was measured using the in-house phantom described above (Figure 1), with the centre of the disc positioned at the centre of the head coil. A multiple echo sequence was used: TR 600, TE 22,60,120. If a ghost image was identified on the image, the ghost level was calculated:

$$\text{Ghost level}(\%) = \frac{I(\text{ghost}) - I(\text{background})}{I(\text{bottle})} \times 100\% \tag{A2}$$

where I is the signal intensity.

Geometric distortion

Geometric distortion was calculated from images of the spherical Siemens phantom used for the SNR measurement. The radius of the test object was calculated using the distance measurement on the scanner console and compared with the actual diameter of 170 mm specified by Siemens. Geometric distortion was also measured from the images of Eurospin TO2, which has four 120 mm long plates arranged in a square. The lengths of these plates were measured on the image using Dispimage. The mean length and coefficient of variation were calculated.

Spatial resolution

Spatial resolution may be assessed either under high contrast conditions with negligible noise contribution, or as a function of object contrast. A qualitative check of resolution can be performed by viewing images of phantoms that have appropriate resolution block patterns, such as the Eurospin TO4 [5]. To obtain a quantitative measure of resolution, the modulation transfer function was determined using Eurospin TO4 placed inside the annulus in the head coil, with the resolution bars parallel to either the x or y direction. The edges of the blocks were then at a small angle θ to the x- and y-axes of the image. The method of Judy [19] was used: since the edge is at a shallow angle to the axis of the pixels, the edge step function is "stretched" over a number of pixels by a factor $f=1/\sin(\theta)$.

From the step function the modulation transfer function (MTF) can be calculated. Unfortunately, the "stretch factor" $f=1/\sin(\theta)$ is very sensitive to angular misalignment: change in f per degree of misalignment is approximately 9%. Using a high resolution (0.35 mm $\times$ 0.35 mm) scan of the phantom, an angle of $10.5^\circ \pm 0.2^\circ$ was measured between the parallel plates and the angled blocks. The actual angle of the blocks to the x-axis was determined to the nearest 0.5° on the images by measuring the angle of the horizontal parallel plates to the y-axis of the image.

A spin echo sequence (TR/TE 500/12, four acquisitions) was used, with field of view 250 mm, 256×256 pixels and 10 mm thick slices. Line profiles were drawn over the blocks in both x and y directions. These were scaled by $\sin(\theta)$, then differentiated to give a line spread function. Fourier transformation of the line spread function gave a MTF. The 50% point of the MTF was calculated. Four acquisitions were averaged to improve SNR, as this processing is sensitive to noise in the image. A further consideration is that the blocks produce zero signal. The images are produced by taking the modulus of a Fourier transform of the raw data, so negative values in the raw data are converted into positive numbers. The data at the edge of the block should oscillate around zero, but after the modulus operation, a skewed distribution with all positive values is produced. The MTF is therefore distorted, and the FWHM is increased. We determined an empirical correction factor of 1.04 by analysing computer generated MTFs. Methods of measuring MTF from the raw data [20] were not considered, since there was no way of accessing raw data from the scanner.